Global metabolomics and lipidomics approaches to probe virus-host interactions

Zhang, Z.

Chapter 3

Altered methionine-sulfone levels are associated with impaired growth in HIV-exposed-uninfected children

Based on

Zhang, Zhengzheng*; Duri, Kerina*; Duisters, Kevin L.W.*; Schoeman, Johannes C.; Chandiwana, Panashe; Lindenburg, Peter; Jaeger, Julia; Ziegler, Susanne; Altfeld, Marcus; Kohler, Isabelle; Harms, Amy; Gumbo, Felicity Z.; Hankemeier, Thomas*; Bunders, Madeleine J. *

Altered methionine-sulfone levels are associated with impaired growth in HIV-exposed-uninfected children

AIDS 37(9):p 1367-1376, July 15, 2023.

*Authors contributed equally

Abstract

To determine immune-metabolic dysregulation in children born to women living with HIV. Longitudinal immune-metabolomic analyses of plasma of 32 pregnant women with HIV (WHIV) and 12 uninfected women and their children up to 1.5 years of age were performed. Using liquid chromatography-mass spectrometry and a multiplex bead assay, 280 metabolites (57 amino acids, 116 positive lipids, 107 signalling lipids) and 24 immune mediators (e.g. cytokines) were quantified. Combinational antiretroviral therapy (cART) exposure was categorized as cART initiation preconception (long), cART initiation postconception up to 4 weeks before birth (medium) and cART initiation within 3 weeks of birth (short). Plasma metabolite profiles differed between HIV-exposed-uninfected (HEU)-children with long cART exposure compared to HIV-unexposed-children (HUU). Specifically, higher levels of methionine-sulfone, which is associated with oxidative stress, were detected in HEU-children with long cART exposure compared to HUU-children. High infant methionine-sulfone levels were reflected by high prenatal plasma levels in the mother. Increased methionine-sulfone levels in the children were associated with decreased growth, including both weight and length. These findings based on longitudinal data demonstrate that dysregulation of metabolite networks associated with oxidative stress in children born to WHIV is associated with restricted infant growth.

Keywords: HIV-1; MTCT; Metabolism; cART; Pediatrics

1. Introduction

The successful roll-out of combinational antiretroviral therapy (cART) has greatly improved health of women living with HIV (WLHIV) and their children and reduced mother-to-child transmission (MTCT) of HIV [1]. Since the introduction of cART, an increasing number of pregnant WLHIV receive cART, including women that initiated cART preconception [2]. Consequently, the population of HIV-exposed-uninfected (HEU) children is steadily increasing [3]. Compared to HIV-unexposed-uninfected (HUU) children, HEU-children, despite being uninfected, experience reduced in utero and postnatal growth, altered cardiac functioning, impaired immunity and enhanced susceptibility to infections [4-6]. In addition, concerns have been raised regarding neurodevelopment in HEU-children [7]. HIV-associated maternal immune activation as well as adverse effects of cART have been suggested to underlie these clinical observations [8,9].

Maternal cART use in pregnancy has been linked to mitochondrial toxicity in HEU-children [9]. Previously, we reported elevated levels of ROS-catalysed lipid peroxidation products in cord blood in HEU compared with HUU-children living in Europe [10]. Emerging data indicate that nutritional status and the local environment, including the microbiome, affect host metabolism limiting translation of findings between different settings [11]. Comprehensive immune-metabolic studies of pregnant women and their children in high HIV prevalence regions are needed to take these factors into account. Furthermore, it is critical to determine whether changes persist after birth and are associated with clinical parameters, such as growth. Here, we report an immune-metabolomic analyses of plasma of HEU and HUU-children from birth up to 1.5 years of age, paired with third trimester maternal blood samples, to assess dysregulation of the metabolism in the child and associated maternal metabolites.

2. Methods

2.1 Study design

The observational University of Zimbabwe Birth Cohort Study in Harare, Zimbabwe, provided the opportunity to analyze plasma samples of WLHIV and uninfected women and their children (**Supplemental Table 1**) [12]. Ethical approval was obtained from the Joint

Research Ethics Committee (JREC) of the University of Zimbabwe and Parirentatwa group of Hospitals (JREC/18/15), the Medical Research Council of Zimbabwe (MRCZ/A/1968), the Research Council of Zimbabwe (SC/9) and ethics committee of the Aerztekammer Hamburg. All study participants provided written informed consent before participation. At enrolment, all women answered a structured questionnaire for assessment of clinical and socio-demographic characteristics. Gestational age was calculated based on the last day of menstruation. The standard of care for all pregnant WLHIV to prevent HIV-MTCT in Zimbabwe during the study period consisted of TENOLAM-E (tenofovir, lamivudine and efavirenz). Duration of cART use was categorized as long (initiation preconception), medium (initiation post conception up to 4 weeks before birth), and no/short (initiation <3 weeks until before delivery). According to national guidelines exclusive breastfeeding is encouraged during the first six months of life, afterwards appropriate complementary foods are advised to be added to breastfeeding. Blood samples were collected at enrolment from mothers and infants at delivery and during follow-up in the neonatal period ("NN", within 14 days of life birth), early infancy ("EI", ⩽6 months) and late infancy ("LI", >6 months). HIV-1 infection was assessed using a 1.5 Roche Amplicor HIV-1 proviral DNA PCR kit (Roche Diagnostics Incorporation, Branchburg, New Jersey) performed on dried blood spots within the first 10 days of life, and regular intervals up to 72 weeks or until cessation of breast feeding, whichever came first [12]. All children were confirmed to be HIV-1-negative.

2.2 Metabolomic and soluble immune mediator profiling

Targeted metabolomics analyses for amines, signalling lipids and positive lipids (total of 280 metabolites), were performed using standard operating procedures described previously [13-15]. Samples for amines, signalling lipids and positive lipids were analyzed using the ultrahigh performance liquid chromatography system coupled to mass spectrometers (SCIEX QTRAP 6500, 6500+, Triple TOF 6600, respectively). A multiparameter multiplex bead assay (Invitrogen) was used to measure plasma levels of 24 cytokines, chemokines and growth factors according to the manufacturer's instructions. The detailed procedures **and target compound lists are provided in the Supplemental Methods.**

2.3 Statistical analysis

Profiled biochemicals were assessed for quality and preprocessed as described in Supplemental Methods. Sample size details on included category intersections are listed in supplemental Table 1. Given its limited sample size, the children with no or short cART exposure were excluded from the main regression analysis and were instead used as independent validation set. Biochemical dynamics for the medium and long exposure groups were compared against HUU-children using main time effects and exposure x time interaction effects in a univariate Linear Mixed Model [16]. The longitudinal dependence between measurements from the same infant was taken into account, as were potential confounders: sex, birth weight centile, gestational age of the child and the mother's BMI upon study entry. Biochemicals for which at least one overall exposure group difference survived a resampling-based FDR multiple testing procedure were considered further [17]. We detected the lowest 20 raw P-values to be smaller than 0.009 and controlled below a false discovery rate (FDR) threshold of q-value < 0.17. This false positive control delivered robust inference when compared against other multiple testing procedures (**Supplemental Table 2**). To unravel temporal dynamics, statistical significance of exposure x time interaction effects in these shortlisted models was assessed using post-hoc Wald tests, and relevant comparisons were made to the maternal sample using paired t-tests. Details are included in **Supplemental Methods**. To interpret these findings, Pearson correlations were used to assess associations between neonatal metabolites and maternal cytokines, as well as metabolites and cytokines in late infancy. A coefficient of 0.5 was considered to indicate moderate to high relevance [18] and these correlations were statistically tested (H0: $r = 0$ vs H1: $r \neq 0$) using the cor.test function from the stats package (version 4.0.2) in R. Further, a growth analysis based on a reference population of sex-specific WHO standardized Z-scores on Weight-for-age (WAZ), Height-for-age (HAZ) and Head circumference-for-age (HCAZ) [19] was used to correlate metabolites to growth parameters.

3. Results

3.1 Patient demographics

In the analyses 44 women and their children were included. The maternal and child characteristics are shown in **Supplemental Table 3**. Duration of cART differed between the HIV-infected women and was associated with viral load, mid-upper arm circumference,

systolic blood pressure, total protein (TP) and high-density lipoprotein (HDL). However, all WLHIV had a CD4+ T cell count exceeding 300 × 106 cells/L, indicating women included were not severely immune suppressed. HEU-children and HUU-children furthermore had a similar distribution with regards to gestational age, birth weight, APGAR scores at 5 minutes, mode of delivery, sex and duration of breastfeeding. There were no differences in breastfeeding observed between the different cART exposure groups.

3.2 Maternal HIV and cART exposure have long-term effects on metabolic networks in children

To determine the immune-metabolic perturbations associated with HIV and cART exposure in children and mothers, plasma samples from 32 WLHIV and 12 uninfected mothers and their children were analysed, using targeted metabolomics approaches and a multiplex bead assay. In total 280 metabolites, including 57 amino acids, 116 positive lipids and 107 signalling lipids, as well as 24 immune mediators (e.g. cytokines), were assessed in a univariate Linear Mixed Model to identify long-term metabolic changes associated with HIV and cART exposure duration. **Table 1** lists the top 20 metabolites with raw unadjusted p-value< 0.05, including several sulphur-containing amino acids, sphingolipids, prostaglandins and glycerophospholipids. Methionine-sulfone showed the strongest association with cART duration (q-value <0.05). An additional six metabolites, phosphatidylcholine (PC) (38:3), ceramides (Cer) Cer(d18:1/23:0) and Cer(d18:1/22:0)), sphingomyelin (SM) (d18:1/16:1) and lyso-phosphatidylethanolamine (LPE) (20:3) were identified with a q-value of < 0.15 in association with cART duration. These metabolites are shown in the context of four relevant pathways in **Figure 1**.

The top 20 metabolites for further analysis, allowing us to consider metabolites from the same chemical class or involved in the same pathway. To identify whether more metabolites from pathway were affected metabolites up to a q-value of 0.17 are shown resulting in a total 20 metabolites. Taken together, maternal cART duration during pregnancy was associated with an altered metabolic profile in HEU-children.

Table 1. Top 20 metabolites with most significant overall group - group differences from linear mixed model.

Order	Metabolites	Medium-cART-HEU vs HUU	Long-cART-HEU vs HUU	Long-cART-HEU vs Medium-cART-HEU
1	Methionine-sulfone	0.019	0.000 ¥¥¥	0.007
2	PC(38:3)	0.602	0.001 ¥¥	0.043
3	Cer(d18:1/23:0)	0.190	0.000 ¥	0.306
4	SM(d18:1/16:1)	0.012	0.001 ¥	0.430
5	LPE(20:3)	0.328	0.001 ¥	0.140
6	Cer(d18:1/22:0)	0.130	0.001 ¥	0.179
7	SM(d18:1/23:1)	0.024	0.001 ¥	0.632
8	PC(38:4)	0.142	0.003	0.624
9	11β-PGE_2	0.035	0.004	0.459
10	LPI(16:1)	0.116	0.006	0.600
11	LPE(16:1)	0.010	0.005	0.698
12	Cysteine	0.253	0.003	0.003
13	CE(18:3)	0.078	0.004	0.097
14	TG(58:10)	0.038	0.003	0.193
15	PE(36:4)	0.262	0.006	0.077
16	S-Methylcysteine	0.005	0.005	0.375
17	SM(d18:1/24:2)	0.105	0.008	0.381
18	Cer(d18:1/24:0)	0.231	0.004	0.242
19	LPE (22:5)	0.486	0.006	0.202
20	DGLEA	0.061	0.009	0.645

Columns contain raw P-values on respective comparison Medium-cART-HEU vs HUU, Long-cART-HEU vs HUU and Long-cART-HEU vs Medium-cART-HEU groups. ¥ indicates FDR-controlled statistical significance under resampling-based q-values: ¥¥¥q <0.05, ¥¥ q< 0.10, ¥q<0.15. PC: phosphatidylcholines; Cer: ceramide; SM, sphingomyelin; LPE: lysophosphatidylethanolamine; 11β-PGE2: 11β-prostaglandin E2; LPI: lysophosphatidylinositol; CE: cholesterol ester; PE: phosphatidylethanolamine; TG: triglyceride; DGLEA: dihomo-γ-linolenic acid; cART: combinational antiretroviral therapy; HEU: HIV-exposed-uninfected; HUU: HIV-unexposed-uninfected.

3.3 Levels of metabolites indicating oxidative stress are associated with prenatal cART exposure in HEU-children

Several biomolecules produced upon oxidative stress, including amino acids in cysteine and methionine metabolism were increased in HEU-children and associated with maternal cART duration (**Figure 1A**). Specifically, increased levels of methionine-sulfone were observed in HEU-children with long cART exposure compared to the HUU and HEU-

children with medium cART exposure (**Figure 1**). Methionine-sulfone is the result of increased in utero oxidation by ROS of methionine, and is associated with the loss of methionine anti-oxidant and inflammatory activity [20]. In line, there was a trend towards higher methionine levels in its unoxidized form in HUU-children (**Figure 1, Supplemental Figure 1**). HEU-children with medium cART exposure displayed less pronounced changes in methionine-sulfone levels during infancy compared to HEU-children with long cART exposure. Mothers of children with long ART exposure had lower viral loads and higher CD4+ T cell counts suggesting reduced HIV-associated disease compared to women initiating cART during pregnancy. The increased levels of methionine-sulfone detected in HEU-children with long cART exposure therefore are more likely associated with cART duration rather than the maternal HIV infection and immune consequences. This was supported by observations in HEU-children with no or short cART-exposure, which had similar lower levels of methionine-sulfone to children born to women who initiated cART during pregnancy (**Supplemental Figure 2**).

Cysteine, also a sulfur-containing amino acid, was showed an increasing trend in HEU-children with long cART-exposure compared to HUU-children. Cysteine is upregulated to reduce oxidative stress [21]. The antioxidant S-methylcysteine, the product of post-translational methylation of cysteine, showed a decreasing trend compared to cysteine, indicating that cysteine synthesis is enhanced in HEU-children with long-cART exposure (**Figure 1, Supplemental Figure 1).** Furthermore, increased levels of 11β-PGE_2 (P=0.007), a PGE_2 isomer, were detected in HEU-children with long cART exposure compared to the HUU-children (**Table 1, Supplemental Figure 1 and 3**). Prostaglandins are produced upon lipid oxidation induced by ROS or enzymatic catabolism of Arachidonic Acid (**Figure 1D**). This class of lipids is well-known for the induction of labor [22,23]. In sum, metabolic changes, indicative of increased oxidative stress, were observed in HEU-children whose mothers had initiated cART prior to conception.

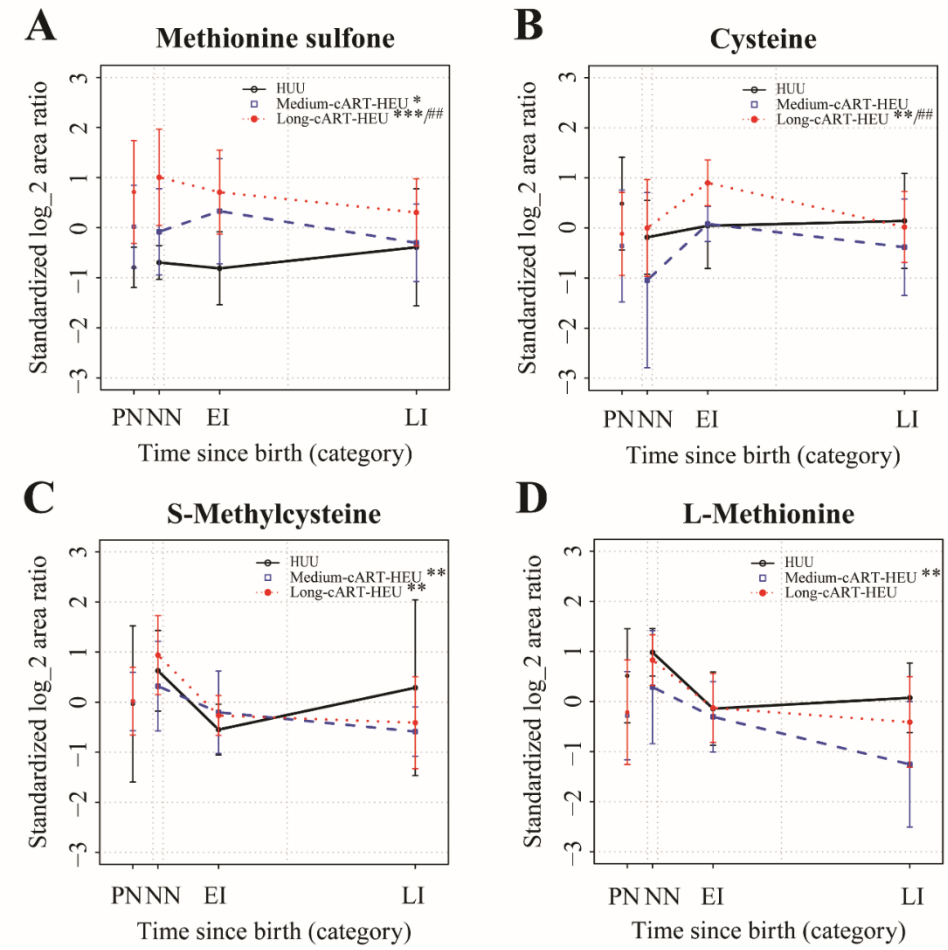

Figure 1: Longitudinal trajectories of sulphur containing amino acids in children. Longitudinal trajectories of (a) methionine-sulfone and three related amino acids ((b) cysteine, hit12; (c) S-methyl cysteine: hit16; (d) L-methionine: hit 75 from the main model) in children and their paired maternal prenatal (PN) samples. The points represent the means of the standardized, log2 area ratios per age category for the exposure groups (black circles represent HUU-children, blue squares represent children in medium-Cart HEU group and red circles represent children in long-cART-HEU group) (age categories: NN: neonate; EI: early infancy; LI: late infancy). The lines connecting the points are interpolations. The maternal prenatal "PN" exposure group means are included as disconnected points at the left of each figure. Represent the corresponding significance level of the raw P-value of group comparisons to HUU from the univariate linear mixed model in the infant cohort (***P<0.001, **P<0.01, *P<0.05); #represent the corresponding significance level of the raw P-value of group comparisons to medium-cART-HEU group from the univariate linear mixed model in the infant cohort (##P<0.01, #P<0.05). The specific raw P-values are further more listed in **Table 1**.

3.4 Glycerophospholipid levels are increased in HEU-children with long cART-exposure

Lipid dysregulation is frequently observed in cART treated HIV-infected individuals [24]. Several species involved in glycerophospholipid metabolism (**Figure 1B**), including PCs and LPEs, were increased in HEU-children with long cART exposure compared to HEU-children with medium cART exposure or HUU-children (**Table 1**). Glycerophospholipids are the most abundant complex lipids and function as building blocks of cellular membranes and signalling molecules [25]. PC(38:3) and LPE(20:3) were increased in HEU-children with long cART exposure compared to the HUU-children (**Figure 2**) with 5 related glycerophospholipids identified in the top 20 of the overall model. Additional analyses of glycerophospholipids at the specific time points indicated that glycerophospholipids (**Supplemental Figure 1**) were specifically increased in early infancy in HEU-children with long cART exposure compared to the HUU-children, and levels attenuated to normal in late infancy.

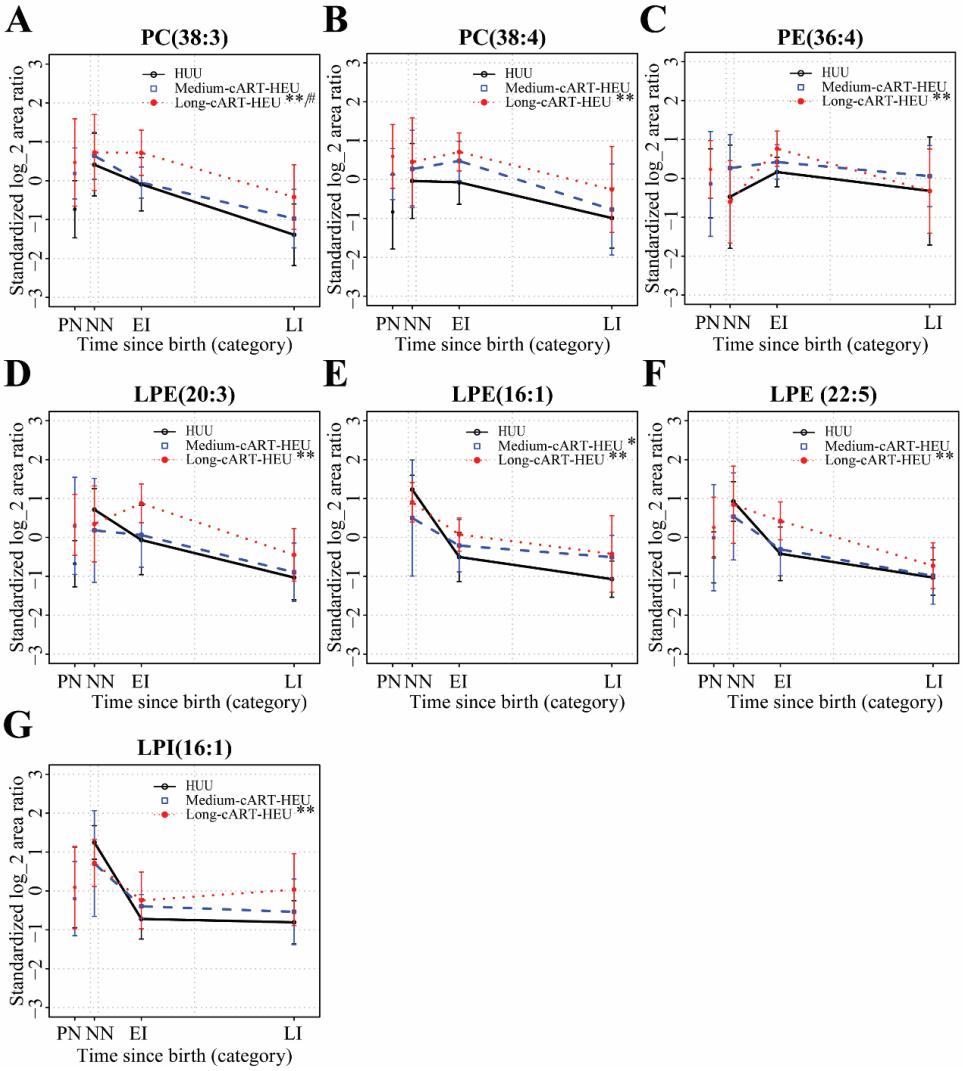

Figure 2: Longitudinal trajectories of glycerophospholipids in children. Longitudinal trajectories of glycerophospholipids((a-g) all within top 20 hits from the main model) in children and their paired maternal prenatal (PN) samples. The points represent the means of the standardized, log2 area ratios per age category for the exposure groups (black circles represent HUU-children, blue squares represent children in medium-Cart HEU group and red circles represent children in long-cART-HEU group) (age categories: NN: neonate; EI: early infancy; LI: late infancy). The lines connecting the points are interpolations. The maternal prenatal "PN" exposure group means are included as disconnected points at the left of each figure. Represent the corresponding significance level of the raw P-value of group comparisons to HUU from the univariate linear mixed model in the infant cohort (***P<0.001, **P<0.01, *P<0.05); #represent the corresponding significance level of the raw P-value of group comparisons to medium-cART-HEU group from the univariate linear

mixed model in the infant cohort (##P<0.01, #P<0.05). The specific raw P-values are further more listed in **Table 1**. LPE, lysophosphatidylethanolamine; LPI, lysophosphatidylinositol; PC, phosphatidylcholines; PE, phosphatidylethanolamine.

3.5 Remodelling of the sphingomyelin-ceramides metabolism in HEU-children with long cART exposure

Ceramides, the precursors of all complex sphingolipids, are potent signalling molecules and furthermore function as building blocks of neuronal membranes [26]. The sphingolipid/ceramide profile differed in HEU-children with long-cART exposure compared to HUU-children (Figure 1C). Specifically, two ceramides (Cer(d18:1/23:0) and Cer(d18:1/23:1); q-value<0.12) and two sphingomyelins (SM(d18:1/16:1) and SM(d18:1/23:1); q-value <0.13) displayed altered levels in HEU-children with long cART exposure compared to HUU-children (Table 1). The top 20 included an additional ceramide and sphingomyelin with differential levels observed between the groups. From birth, ceramides and sphingomyelins followed a similar trajectory, showing increased levels in early infancy in HEU-children with long cART exposure compared to HUU-children (**Figure 3, Supplemental Figure 1 & Figure pathway 2 or 3**). Taken together, these findings suggested an altered sphingolipid/ceramide metabolism in HEU-children with long cART exposure although the difference is not statistically significant after multiple testing **correction.**

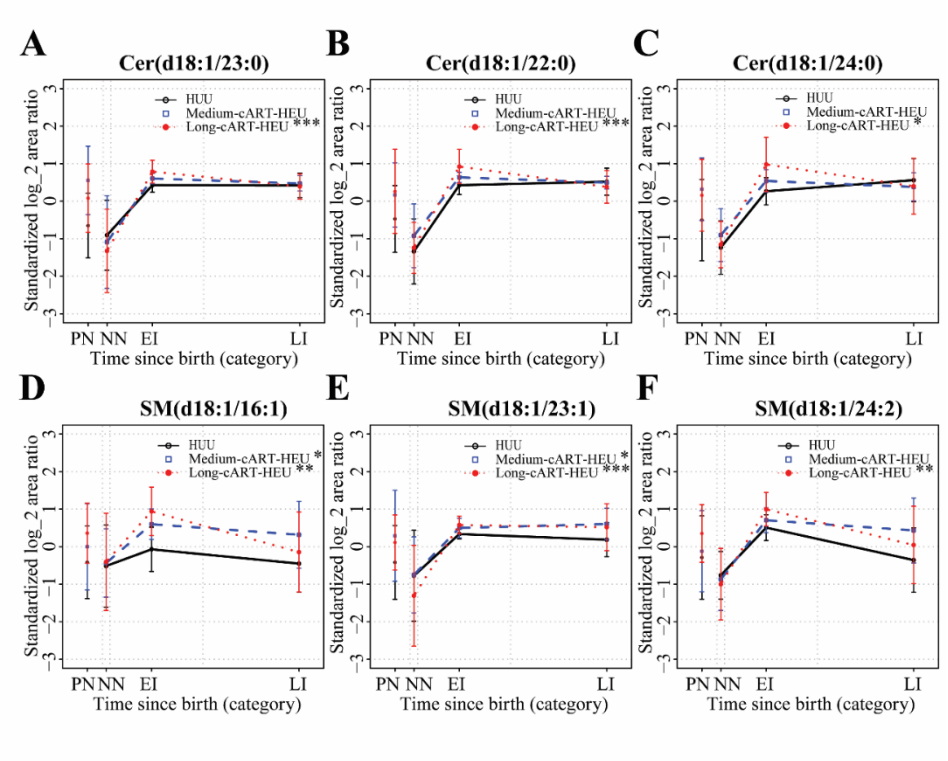

Figure 3: Longitudinal trajectories of sulphur containing amino acids in children. Longitudinal trajectories of sphingolipids ((a-f) all within the top 20 hits from the main model) in children and their paired maternal prenatal (PN) samples. The points represent the means of the standardized, log2 area ratios per age category for the exposure groups (black circles represent HUU-children, blue squares represent children in medium-Cart HEU group and red circles represent children in long-cART-HEU group) (age categories: NN: neonate; EI: early infancy; LI: late infancy). The lines connecting the points are interpolations. The maternal prenatal "PN" exposure group means are included as disconnected points at the left of each figure. Represent the corresponding significance level of the raw P-value of group comparisons to HUU from the univariate linear mixed model in the infant cohort (***P<0.001, **P<0.01, *P<0.05); #represent the corresponding significance level of the raw P-value of group comparisons to medium-cART-HEU group from the univariate linear mixed model in the infant cohort (##P<0.01, #P<0.05). The specific raw P-values are further more listed in **Table 1**.

3.6 Infant metabolic dysregulation is associated with maternal metabolic dysregulation

Next, we investigated whether maternal methionine-sulfone levels predicted infant methionine-sulfone levels. In line with the data presented in Figure 1, maternal methionine-

sulfone levels reflected infant levels, as no significant differences were observed between maternal and infant methionine sulfone levels (t-test: maternal to infant HUU: P=0.406; maternal to infant medium-HEU: P=0.972; and maternal to infant long-HEU: P=0.261, respectively), indicating that the maternal methionine-sulfone levels are an adequate predictor of altered levels in the child. These findings suggest that metabolic dysregulation in the mother associated with cART duration underlies metabolic changes in the infant, however this does not rule out that maternal immune activation in the mother may impact the child as well. To this end, we performed immune-metabolic correlation analyses between maternal immune mediators and infant metabolites at birth, using a correlation coefficient cut-off of (r) $\geqslant 0.5$ or $\leqslant -0.5$ [18]. Methionine-sulfone was not correlated with CD4+ T cell counts, viral load, or maternal plasma cytokine levels (**Supplemental Figure 4, Supplemental Table 4**). Infant L-methionine levels were correlated to maternal CD4+ T cell counts and infant cysteine with maternal viral load indicating that next to the strong association of maternal cART duration with methionine-sulfone in the infant, potential effects of maternal HIV on methionine metabolism cannot be excluded. Furthermore, infant ceramides and sphingomyelins were negatively associated with maternal cytokines, including IL-2 and IL-1β. To assess whether infant metabolic dysregulation after 6 months of age was associated with infant immune mediators, infant metabolites were correlated to infant immune parameters. However, few infant metabolites correlated to infant immune parameters, suggesting that metabolic dysregulation in children may not have long-term effects on soluble immune mediators. Specifically, no significant associations were observed between infant soluble immune mediators and methionine-sulfone levels (**Supplemental Figure 5 & Supplemental Table 5**). In sum, these findings suggest that methione-sulfone dysregulation in HEU-infants is associated with metabolic dysregulation in the mother rather than maternal immune dysregulation.

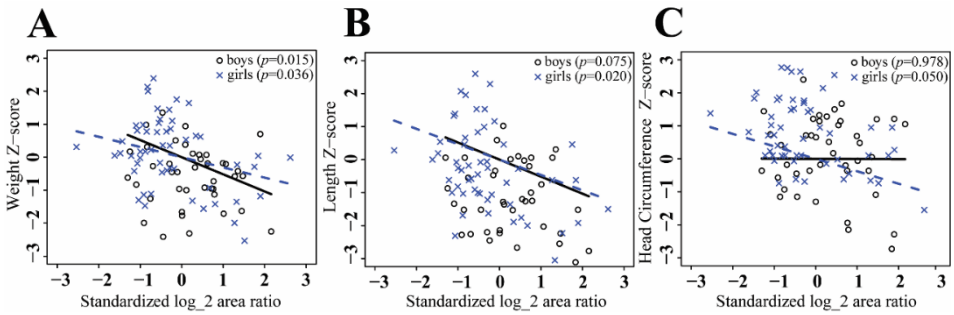

Figure 4: Correlations of methionine-sulfone with weight Z-score (a), length Z-score (b), and head circumference Z-score (c). The points represent standardized log2 area ratios across all longitudinal infant samples for children in all groups included in the main model (black circles for boys; blue crosses for girls). Regression lines and associated mixed model P-values included for boys (black solid line) and girls (blue dashed line).

3.7 Increased levels of methionine-sulfone are associated with decreased infant growth

Associations with maternal immune dysregulation and cART have been suggested to underlie decreased growth in HEU-children [6]. As methionine-sulfone dysregulation is a characteristic of oxidative stress and reduced energy production [20], we determined whether infant methionine-sulfone levels were associated with infant growth. The association between methionine-sulfone and height, weight and head circumference was investigated using a linear regression model adjusted for BMI, gestational age, and sex. Growth parameters were expressed as Z-scores according to WHO definitions [19]. Elevated infant methionine-sulfone levels negatively correlated to weight (P=0.015) in boys, and reduced weight (P=0.036) and length (P=0.020) in girls (Figure 4). There was a trend towards reduced head circumference in girls with higher methionine-sulfone levels. In sum, metabolic dysregulation with increased levels of methionine-sulfone in infants are associated with decreased postnatal growth.

4. Discussion

Although the number of HEU-children is rapidly increasing concerns remain regarding the long-term consequences of maternal HIV and cART exposure. Here, we demonstrated based on longitudinal immune-metabolomics analyses of Zimbabwean mother-child pairs long-term disrupted metabolic functioning in HEU-children. In particular, children born to WLHIV who had initiated cART prior to conception exhibited metabolic changes and

increased levels of methionine-sulfone. Increased infant methionine-sulfone levels were associated with decreased growth. Methionine-sulfone levels in the child correlated to those in the mother suggesting it could be directly transferred to the infant transplacentally [1] or via breastfeeding [2,3]. This may offer a potential novel clinical correlate for risk of impaired growth in HEU-children.

cART during pregnancy dramatically improves health in women and children [8], however some studies have suggested that initiation prior to conception may increase the risk of adverse effects [27]. In this study methionine-sulfone was especially elevated in HEU-children born to women who had initiated cART prior to conception. This is in line with previous findings showing increased methionine-sulfone levels in HIV-infected persons or patients with HIV on long-term cART compared to uninfected individuals [28]. Oxidized-methionine residues and their reduction by the Msr system impair the resilience of antioxidant defense, which is critical to main cellular homeostasis[29]. Although several ARTs are known for affecting mitochondrial dysfunction through the inhibition of DNA pol-γ[30], efavirenz, which was used in the maternal cART regimen in this study, is less well-known for its mitochondrial toxicity. Recent studies however showed increased levels of metabolites associated with oxidative stress in HIV-infected individuals treated with efavirenz [31]. Furthermore, elevated prostaglandin levels were observed in women who initiated cART prior to conception, and in their children. Prostaglandins are potent inducers of labour and the findings presented here may suggest their involvement of oxidative stress and labour induction [23]. The unique comparison in this longitudinal cohort provided the opportunity to compare different cART exposure times as well as a small group of children with no or less than 3 weeks cART exposure. The latter showed more similar methionine-sulfone levels to HUU-children and HEU-children with medium cART exposure and compared to HEU-children with long cART exposure. Furthermore, maternal CD4+ T cell count, viral load or maternal plasma cytokines, were not strongly associated with methionine-sulfone. Considering that long-term cART is critical for the mother's health further studies are needed to identify potential pathways that can be targeted to reduce adverse effects of cART. Furthermore, alternative cART regimens are increasingly used. Longitudinal studies are needed to assess whether these alternative cART regimens have a reduced potential to perturb the maternal and infant metabolism. Taken together, increased

methionine-sulfone levels indicative of oxidative stress are observed in HEU-children born to WLHIV who initiated cART prior to conception.

Altered sphingolipid/ceremide metabolism was furthermore observed in children born to HIV- infected women. Ceramides, the precursors of all complex sphingolipids, are potent signalling molecules and well-known biomarkers for cardiovascular diseases [32]. Sphingolipid metabolism is furthermore critical for efficient neuronal functioning [33]. Ceramide intracellular levels are fine-tuned and alteration of the sphingomyelin-ceramide signalling profile are associated with the development of age-related, neurological and neuroinflammatory diseases [33-35]. Although still under debate, studies suggest that HEU-children are at risk of impaired neurological development [7]. The altered sphingolipid metabolism observed in this study may contribute to altered neural development in HEU-children. These observations require further studies to unravel the underlying mechanisms. Lipid metabolism was less affected than reported in previous studies in HEU-children and in HIV-infected patients [36]. This may reflect the less lipid toxic profile of TENOLAM versus protease inhibitors [10,28].

Decreased postnatal growth is an important clinical parameter of child health and associated with increased morbidity and mortality [37]. HEU-children are smaller for gestational age and have an increased risk for reduced postnatal growth [6,38]. Our data suggests that that increased oxidative stress may have consequences for infant growth. As maternal methionine-sulfone levels were similar to the children, maternal methionine-sulfone furthermore may provide a new biomarker for decreased growth during pregnancy in mothers and during follow-up in HEU-children. These observations require further studies to assess the validity of maternal and infant methionine-sulfone to predict postnatal growth.

In conclusion, our findings demonstrated metabolic dysregulation indicating increased oxidative stress in WLHIV and their uninfected children, which is associated with timing of cART initiation and decreased growth. Future studies are needed to uncover the mechanisms underlying long-term mitochondrial dysregulation in HEU-children in a larger cohort and inform on interventions that can restore metabolic functioning in WLHIV and children to promote healthy development.

Acknowledgements

The authors would like to thank the participants of the UZ-CHS birth cohort study and the research support team for their commitment including Dr. G Kandawasvika, Dr. P Kuona, Dr. S Chimhuya (Paediatrics and Child Health Unit, Dr. A Ziruma (Obstetrics and Gynaecology Unit), Mr Privilege Munjoma (Immunology Unit). Zhengzheng Zhang would like to acknowledge the China Scholarship Council (CSC, No.201608140084). The cohort is registered at www.clinicaltrials.gov.trial registration number: NCT04087239.

Author contributions:

KD, PC and FZG collected of epidemiological data. MJB, KD, TH and JCS designed the study and methodological approaches. ZZ and SZ performed experiments. KLWD performed statistical analyses. ZZ, KD, KLWD, JCS, MJB, JJ, PL, IK, AH, MA and FZG performed interpretation of the data. ZZ, KD, KLWD, JCS, MJB., PL, IK, AH, MA and FZG drafted the manuscript. MJB and TH supervised the study.

Funding: This work was supported by the Wellcome Trust under the University Of Zimbabwe College Of Health Sciences Southern Africa Consortium for Research Excellence (SACORE) [087537/F/08/A], the Deutsche Forschungsgemeinschaft (DFG) [BU 3630/2-1], and the Netherlands X-omics Initiative and NWO [184.034.019]. None of the funding bodies were be involved in the study design, data collection, data analysis, interpretation of findings and/ or manuscript writing. Potential conflicts of interest. The authors: No reported conflicts of interest.

References

1 Townsend CL, Cortina-Borja M, Peckham CS, de Ruiter A, Lyall H, Tookey PA. Low rates of mother-to-child transmission of HIV following effective pregnancy interventions in the United Kingdom and Ireland, 2000-2006. *AIDS*. 2008; 22:973-981.

2 UNAIDS. Number of people living with HIV. Available at: http://aidsinfo.unaids.org/. Accessed 5 May 2022.

3 UNAIDS. Number of HIV-exposed children who are uninfected. Available at: http://aidsinfo.unaids.org/. Accessed 5 May 2022.

4 Adler C, Haelterman E, Barlow P, Marchant A, Levy J, Goetghebuer T. Severe infections in HIV-exposed uninfected infants born in a European Country. *PLoS One*. 2015; 10(8):e0135375.

5 Le Roux SM, Abrams EJ, Donald KA, Brittain K, Phillips TK, Zerbe A, et al. Infectious morbidity of breastfed, HIV-exposed uninfected infants under conditions of universal

antiretroviral therapy in South Africa: a prospective cohort study. *Lancet Child Adolesc Health*. 2020; 4:220-231.

6 Le Roux SM, Abrams EJ, Donald KA, Brittain K, Phillips TK, Nguyen KK, et al. Growth trajectories of breastfed HIV-exposed uninfected and HIV-unexposed children under conditions of universal maternal antiretroviral therapy: a prospective study. *Lancet Child Adolesc Health*. 2019; 3:234-244.

7 Toledo G, Côté HCF, Adler C, Thorne C, Goetghebuer T. Neurological development of children who are HIV-exposed and uninfected. *Dev Med Child Neurol*. 2021; 63:1161-1170.

8 Goetghebuer T, Smolen KK, Adler C, Das J, McBride T, Smits G, et al. Initiation of antiretroviral therapy before pregnancy reduces the risk of infection-related hospitalization in human immunodeficiency virus-exposed uninfected infants born in a high-income country. *Clin Infect Dis.* 2019; 68:1193-1203.

9 Ajaykumar A, Zhu M, Kakkar F, Brophy J, Bitnun A, Alimenti A, et al. Elevated blood mitochondrial DNA in early life among uninfected children exposed to human immunodeficiency virus and combination antiretroviral therapy in utero. *J Infect Dis*. 2021; 223:621-631.

10 Schoeman JC, Moutloatse GP, Harms AC, Vreeken RJ, Scherpbier HJ, Van Leeuwen L, et al. Fetal metabolic stress disrupts immune homeostasis and induces proinflammatory responses in human immunodeficiency virus type 1-And combination antiretroviral therapy-exposed infants. *J Infect Dis*. 2017; 216:436-446.

11 Rouse BT, Sehrawat S. Immunity and immunopathology to viruses: what decides the outcome? *Nat Rev Immunol*. 2010; 10:514-26.

12 Duri K, Gumbo FZ, Munjoma PT, Chandiwana P, Mhandire K, Ziruma A, et al. The university of zimbabwe college of health sciences (UZ-CHS) birth cohort study: rationale, design and methods. *BMC Infect Dis*. 2020; 20:725.

13 Noga MJ, Dane A, Shi S, Attali A, van Aken H, Suidgeest E, et al. Metabolomics of cerebrospinal fluid reveals changes in the central nervous system metabolism in a rat model of multiple sclerosis. *Metabolomics*. 2012; 8:253-263.

14 Schoeman JC, Harms AC, van Weeghel M, Berger R, Vreeken RJ, Hankemeier T. Development and application of a UHPLC–MS/MS metabolomics based comprehensive systemic and tissue-specific screening method for inflammatory, oxidative and nitrosative stress. *Anal Bioanal Chem*. 2018; 410:2551-2568.

15 Hu C, van Dommelen J, van der Heijden R, Spijksma G, Reijmers TH, Wang M, et al. RPLC-lon-trap-FTMS method for lipid profiling of plasma: method validation and application to p53 mutant mouse model. *J Proteome Res.* 2008; 7:4982-4991.

16 McCullogh CE, Searle SR., Neuhaus JM. Generalized, Linear, and Mixed Models 2nd ed., New York, NY John Wiley & Sons; 2008; 157-187.

17 Yekutieli D, Benjamini Y. Resampling-based false discovery rate controlling multiple testing procedures for correlated test statistics. *J Stat Plan Inference*. 1999; 82:171-196.

18 Hinkle DE, Wiersma W, Jurs SG. Applied statistics for the behavioral sciences. *Boston: Houghton Mifflin*. 2003. pp:108-112.

19 WHO Multicentre Growth Reference Study Group. WHO Child Growth Standards: Length/height-for-age, weight-for-age, weight-for-length, weight-for-height and body mass index-for-age: Methods and development. *Geneva: World Health Organization*. 2006.

20 Unnikrishnan MK, Rao MNA. Antiinflammatory activity of methionine, methionine sulfoxide and methionine sulfone. *Agents Actions.* 1990; 31:110-112.

21 Van der Reest J, Lilla S, Zheng L, Zanivan S, Gottlieb E. Proteome-wide analysis of cysteine oxidation reveals metabolic sensitivity to redox stress. *Nat Commun*. 2018; 9:1581.

22 Maseda D, Ricciotti E, Crofford LJ. Prostaglandin regulation of T cell biology. *Pharmacol Res*. 2019; 149:104456.

23 Alfirevic Z, Keeney E, Dowswell T, Welton NJ, Dias S, Jones LV. Labour induction with prostaglandins: a systematic review and network meta-analysis. *BMJ*. 2015; 350:h217.

24 Fontas E, van Leth F, Sabin CA, Friis-Møller N, Rickenbach M, d'Arminio Monforte A, et al. Lipid profiles in HIV-infected patients receiving combination antiretroviral therapy: are different antiretroviral drugs associated with different lipid profiles? *J Infect Dis*. 2004; 189:1056-74.

25 Fernandis AZ, Wenk MR. Membrane lipids as signaling molecules. *Curr Opin Lipidol*. 2007; 18:121-8.

26 Hannun YA, Obeid LM. Principles of bioactive lipid signalling: lessons from sphingolipids. *Nat Rev Mol Cell Biol.* 2008; 9:139-50.

27 Theron G, Brummel S, Fairlie L, Pinilla M, McCarthy K, Owor M, et al. Pregnancy outcomes of women conceiving on antiretroviral therapy (ART) compared to those commenced on ART during pregnancy. *Clin Infect Dis.* 2021; 73:e312-e320.

28 Babu H, Sperk M, Ambikan AT, Rachel G, Viswanathan VK, Tripathy SP, et al. Plasma metabolic signature and abnormalities in HIV-infected individuals on long-term successful antiretroviral therapy. *Metabolites*. 2019; 9: 210.

29 Agbas A, Moskovitz J. The role of methionine oxidation/reduction in the regulation of immune response. *Curr Signal Transduct Ther*. 2009; 4:46-50.

30 Brinkman K, Smeitink JA, Romijn JA, Reiss P. Mitochondrial toxicity induced by nucleoside-analogue reverse-transcriptase inhibitors is a key factor in the pathogenesis of antiretroviral-therapy-related lipodystrophy. *Lancet*. 1999; 354:1112-1115.

31 Deresz LF, Lazzarotto AR, Manfroi WC, Gaya A, Sprinz E, de Oliveira ÁR, et al. Oxidative stress and physical exercise in HIV positive individuals. *Rev Bras Med Esporte*. 2007; 13: 275-279.

32 McGurk KA, Keavney BD, Nicolaou A. Circulating ceramides as biomarkers of cardiovascular disease: Evidence from phenotypic and genomic studies. *Atherosclerosis*. 2021; 327:18-30.

33 Olsen ASB, Færgeman NJ. Sphingolipids: membrane microdomains in brain development, function and neurological diseases. *Open Biol*. 2017; 7:170069.

34 Nixon GF. Sphingolipids in inflammation: pathological implications and potential therapeutic targets. *Br J Pharmacol.* 2009; 158:982-93.

35 Augé N, Andrieu N, Nègre-Salvayre A, Thiers JC, Levade T, Salvayre R. The sphingomyelin-ceramide signaling pathway is involved in oxidized low density lipoprotein-induced cell proliferation. *J Biol Chem*. 1996; 271:19251-19255.

36 Ramteke SM, Shiau S, Foca M, Strehlau R, Pinillos F, Patel F, et al. Patterns of growth, body composition, and lipid profiles in a South African cohort of human immunodeficiency virus-infected and uninfected children: a cross-sectional study. *J Pediatric Infect Dis Soc*. 2018; 7:143-150.

37 Myatt M, Khara T, Schoenbuchner S, Pietzsch S, Dolan C, Lelijveld N, et al. Children who are both wasted and stunted are also underweight and have a high risk of death: a descriptive epidemiology of multiple anthropometric deficits using data from 51 countries. *Arch Public Health*. 2018; 76:28.

38 Bailey RC, Kamenga MC, Nsuami MJ, Nieburg P, St Louis ME. Growth of children according to maternal and child HIV, immunological and disease characteristics: a prospective cohort study in Kinshasa, Democratic Republic of Congo. *Int J Epidemiol*. 1999; 28:532-540.

SUPPLEMENTARY MATERIAL

Sample Collection

Ten milliters of maternal venous blood was collected at enrolment. Umbilical cord blood and venous blood were obtained at delivery and follow-up visits, respectively. Blood was collected in ethylenediaminetetraacetic acid (EDTA) vacutainer tubes. Plasma was obtained by centrifugation at 5000g for 10 min at 4°C and stored at -20°C.

Metabolomics Analyses

Targeted metabolomics analyses were performed using standard operating procedures based on previously published methods [1-3].

Amines profiling

Five microliters of plasma were spiked with ten microliters of an internal standard solution containing $^{13}C^{15}N$-labeled amino acids. Protein precipitation was carried out by adding five hundred microliters of MeOH to the samples. Samples were analyzed using an ACQUITY ultra performance liquid chromatography system (Waters Chromatography Europe BV, Etten-Leur, The Netherlands) coupled to a Triple Quadrupole Linear Ion Trap instrument (SCIEX QTRAP 6500) using a previously validated method [1].

Positive lipids profiling

Ten microliters of plasma were spiked with calibration and internal standards and extracted using isopropyl alcohol. Samples were analyzed using an ACQUITY ultra performance liquid chromatography system (Waters Chromatography Europe BV, Etten-Leur, The Netherlands) coupled to a quadrupole time-of-flight (SCIEX Triple TOF 6600) [2].

Signaling lipid mediators profiling

One hundred and fifty microliters of plasma were spiked with calibration and internal standards using lipid-liquid extraction. Then the samples were analyzed using Shimadzu

liquid chromatography system coupled to a Triple Quadrupole Linear Ion Trap (SCIEX Q Trap 6500+) [3].

Soluble immunological mediators

Multiplex testing was used to measure chemokines and cytokine levels including B-cell activating factor, B cell-attracting chemokine 1, brain-derived neurotrophic factor, interferon gamma inducible protein10, monokine induced by gamma interferon, monocyte chemo-attractant protein 1, monocyte chemo-attractant protein 3, macrophage inflammatory protein-1β, tumour necrosis factor alpha, matrix metalloproteinase-1, Macrophage migration inhibitory factor, Stem cell factor, interleukin (IL)-1β, IL-2, IL-4, IL-6, IL-10, IL-12p70, IL-17A, IL-27, IL-8, IL-2Rα, cluster of differentiation (CD) 30 and CD40.

Preprocessing lipid and amines data

Quality control procedures were used to monitor the data acquisition quality by adding quality control (QC) samples regularly within each batch, i.e., every 10th study sample. QC samples were prepared by pooling equal volumes of each study sample. An in-house developed tool, mzQuality, was used to correct for batch effects and highlight metabolites with high technical noise, calculated as the relative standard deviation observed in the QC samples**.** Metabolites with a variability lower than 30% and blank measurement effect less than 30% in QC samples (expressed in relative standard deviation, RSD) were considered. In total, 280 metabolites, i.e., 57 biogenic amines, 107 signalling lipid mediators, 116 positively charged lipids) were selected for further data analysis. In case quantifications returned below detection limit, which never exceeded 5% of attempted quantifications for each biochemical, 0.5 times the minimum of the observed area ratios for the respective biochemical was imputed. After imputation, combining infants and their mothers, about 42 thousand metabolomics datapoints were studied across 152 samples. Less than 2% of these datapoints were blanks, assumed to be missing at random.

Analyses of soluble immunological mediators

A total of 24 soluble immunological mediators (mostly cytokines) were measured in 152 samples. Out of these samples, due to limited plasma availability 123 had three technical replicates, four were measured twice, and 27 were measured once. In addition, standards were determined for each immunological mediator on each plate. Of all the attempted quantifications, approximately 6% were extrapolated, 0.2% were above the limit of detection and 17% were below the limit of detection. To account for plate effects, values above the limit of detection were imputed with 2 times the maximum of both the observed values (including extrapolated values) and the highest standard per cytokine per plate. Values below the limit of detection were imputed with 0.5 times the minimum of both the observed values (including extrapolated values) and the lowest standard value per immunological mediator per plate. After imputation, technical replicates (if any) were averaged to obtain a single value per immunological mediator per sample. In total, 3648 datapoints were studied across 152 samples on 24 immunological mediators. Less than 1% of these datapoints were blanks, assumed to be missing at random. In the case of IL-2, IL-17A, IL-1β and IL-12p70 over half of measurements were imputed, and results are to be interpreted with caution for robustness against this imputation strategy. All extrapolated values were included as observed values in the data analysis. To account for plate effects, values above the limit of detection were imputed with 2 times the maximum of both the observed values (including extrapolated values) and the highest standard per cytokine per plate. Values below the limit of detection were imputed with 0.5 times the minimum of both the observed values (including extrapolated values) and the lowest standard value per immunological mediator per plate. After imputation, technical replicates (if any) were averaged to obtain a single value per immunological mediator per sample.

Data preprocessing

After the imputation strategy described in the biochemical preprocessing, data quality was concluded to be sufficiently high to proceed after outlier checks, missing checks, and visual assessment. Measurements were log-2 transformed and standardized by biochemical to mean zero and unit variance for consistent interpretation across compounds. Given the limited number of children with no or short cART exposure, children with no or short cART exposure were excluded from the main regression analysis and were instead used as independent data set showing individual points.

Statistical model estimation

For each biomolecule *j* in 1 to 304, we denote the standardized, log-2 transformed MS area ratio from infant *i* at time *t* by $Y_{i,t}^{(j)}$. Here, standardization is understood as centering to mean zero and rescaling to standard deviation one. The following linear mixed model [4] is estimated in R (version 3.4.3) [5] using the *nlme* package (version 3.1 - 137) [6].

$$Y_{i,t}^{(j)} = b_i^{(j)} + \mu_t^{(j)} + (\delta_1^{(j)} + \gamma_{1,t}^{(j)})Medium_i + (\delta_2^{(j)} + \gamma_{2,t}^{(j)})Long_i + \beta_1^{(j)}Sex_i + \beta_2^{(j)}BWC_i + \beta_3^{(j)}GA_i + \beta_4^{(j)}BMI_i + \varepsilon_{i,t}^{(j)}$$

From now on, the superscript (j) will be dropped from notation and we understand all parameters to be estimated univariately for each biomolecule. The random intercept $b_i \sim N(0, \sigma_b^2)$ accounts for the longitudinal character of the data by introducing dependence between measurements of the same infant. Fixed effects μ_t model the mean of the standardized, log-2 transformed MS area ratios for the HUU reference group over time. Interest goes out to biomolecules with statistically significant average group effects (δ_1 and/or δ_2), potentially including average group x time interactions ($\gamma_{1,t}$ and/or $\gamma_{2,t}$ for *t* equal to early infancy (EI) or late infancy (LI) categories, with $\gamma_{1,0} = \gamma_{2,0} = 0$ imposed at the neonatal (NN) category for statistical identifiability). These effects are controlled against four potential confounders: sex, WHO birth weight centile (BWC), gestational age (GA) and the mother's BMI upon study entry. Finally, the error term $\varepsilon_{i,t}$ is assumed to follow an underlying multivariate normal distribution $\varepsilon_i \sim N(\mathbf{0}, \mathbf{\Sigma})$ with mean vector zero and 3x3 covariance matrix $\mathbf{\Sigma}$. Here, $\mathbf{\Sigma}$ is modeled as diagonal with heterogeneous variances to allow error variance to differ between time categories (NN, EI and LI). An off-diagonal, continuous AR1 structure that accounts for non-equally spaced measurements was not found to contribute to model fit sufficiently.

Hypothesis testing and multiple testing control

The **Results** section describes significant effects based on the statistical model by a two-step approach.

In step one, biochemicals are selected that show at least one significant, overall difference between two exposure groups. To control for false positives as a result of considering a

large number of 304 biochemicals, a resampling-based False Discovery Rate (FDR) correction is used, inspired by Yekutieli and Benjamini [7]. This procedure improves on the FDR-algorithm by Benjamini and Hochberg [8] by taking the dependence structure between biochemicals into account. For instance, in the case of comparing the Medium-HUU overall difference between groups, one is interested in the p-value of a likelihood ratio $\delta_1 = \gamma_{1,1} = \gamma_{1,2} = 0$ against the full statistical model stipulated χ_3^2 distribution under the null hypothesis. The resampling-based procedure controls the FDR under dependence by creating an empirical null distribution of all 304 p-values jointly, using 600 random permutations of the Medium/HUU group membership. Based on this empirical distribution, clustering of false positives informs how to adjust p-values obtained using the original data. These original p-values and their adjustments (known as q values) are shown in Table 2. Importantly, this permutation approach leaves the longitudinal character of our data intact. For further detail, the reader is referred to Supplemental Table 1, which contains a robustness analysis against other multiple testing algorithms to assess sensitivity against our main findings.

In step two, statistical significance at the underlying level of group x time interactions is assessed, but only for those biochemicals that have survived the FDR threshold selection in step one. For instance, to test whether the average difference between the Medium group and the HUU group at time category early infancy (EI) is zero or not, the Wald test statistic is computed:

$$\frac{(\widehat{\delta_1} + \widehat{\gamma_{1,1}}) - 0}{\widehat{\mathrm{Cov}}(\delta_1, \delta_1) + \widehat{\mathrm{Cov}}(\gamma_{1,1}, \gamma_{1,1}) + \widehat{\mathrm{Cov}}(\delta_1, \gamma_{1,1})}$$

a χ_1^2 distribution under the null hypothesis. In the nominator, the hat notation refers to the parameter estimates from the statistical model (for the selected biochemical in question). The (co)variance terms in the denominator follow from the estimated fixed-effect covariance matrix in the *nlme* package (version 3.1 - 137) [6]. The other effect sizes are treated analogously.

Finally, a growth analysis based on WHO reference centiles was conducted to assess associations between the shortlisted biochemicals and growth outcomes. Here, the Z scores

were (separately) modelled in a univariate Linear Mixed Model with a main effect for the respective biochemical and random effect for the infant.

References

1 Noga MJ, Dane A, Shi S, Attali A, van Aken H, Suidgeest E, et al. Metabolomics of cerebrospinal fluid reveals changes in the central nervous system metabolism in a rat model of multiple sclerosis. *Metabolomics*. 2012;8(2):253-263.

2 Schoeman JC, Harms AC, van Weeghel M, Berger R, Vreeken RJ, Hankemeier T. Development and application of a UHPLC–MS/MS metabolomics based comprehensive systemic and tissue-specific screening method for inflammatory, oxidative and nitrosative stress. *Anal Bioanal Chem*. 2018;410(10):2551-2568.

3 Hu C, van Dommelen J, van der Heijden R, Spijksma G, Reijmers TH, Wang M, et al. RPLC-lon-trap-FTMS method for lipid profiling of plasma: Method validation And application to p53 mutant mouse model. *J Proteome Res*. 2008;7(11):4982-4991.

4 McCullogh CE, Searle SR., Neuhaus JM. Generalized, linear, and mixed models 2nd ed. *John Wiley & Sons*. 2008; 157-187.

5 R Core Team. R: A language and environment for statistical computing. R Foundation for Statistical Computing. Vienna, Austria 2017. Available at: https://www.R-project.org.

6 Pinheiro, J., Bates, D., DebRoy, S., Sarkar, D., and R Core Team. nlme: Linear and Nonlinear Mixed Effects Models 2017. Available at: https://CRAN.R- project.org/package=nlme.

7 Yekutieli D, Benjamini Y. Resampling-based false discovery rate controlling multiple testing procedures for correlated test statistics. *J Stat Plan Inference*. 1999;82:171-196.

8 Y. Benjamini and Y. Hochberg. Controlling the false discovery rate: a practical and powerful approach to multiple testing. *J R Stat Soc Series B Stat Methodol*. 1995; 57(1): 289-300.

Supplemental Table 1. Longitudinal sample distribution

			Time since birth			
			[-124,-1]	*[0,4]*	*[36, 185]*	*[187, 548]*
		Group	PN*	NN	EI	LI
cART exposure	*[0,0]*	HUU	12	**12**	**12**	**11**
	[10,20]	Short-cART-HEU	6	5	2	3
	[24, 259]	Medium-cART-HEU	12	**9**	**7**	**10**
	[301, 2181]	Long-cART-HEU	14	**10**	**14**	**13**
		Total (n)	44	36	35	37

Observed category ranges *[min, max]* in days and intersection sample sizes in unique counts resulting from categorization of cART exposure and collection time into groups. Sample sizes (bold) from the orange area of the table are included in the main analysis.
Note: * Prenatal samples collected in mothers.
cART: combinational antiretroviral therapy; PN: Prenatal; NN: Neonatal; EI :Early Infancy; LI: Late Infancy.

Supplemental Table 2. Robustness analysis on multiple testing correction.

	raw	**FDR**	FDR	FDR	FDR	FWER	FWER	FWER
Biochemical	*p*-value	**resampling based**	Benjamini-Yekutieli	Benjamini-Hochberg	Li& Ji*	Bonferroni	Westfall& Young	Li &Ji*
Methionine-sulfone	0.00	**0.02**	0.00	0.00	0.00	0.00	0.05	0.00
PC(38:3)	0.00	**0.10**	0.32	0.05	0.02	0.31	0.43	0.04
Cer(d18:1/23:0)	0.00	**0.11**	0.32	0.05	0.01	0.13	0.26	0.02
SM(d18:1/16:1)	0.00	**0.11**	0.38	0.06	0.02	0.43	0.50	0.06
LPE(20:3)	0.00	**0.11**	0.32	0.05	0.02	0.30	0.42	0.04
Cer(d18:1/22:0)	0.00	**0.12**	0.32	0.05	0.02	0.21	0.34	0.03
SM(d18:1/23:1)	0.00	**0.12**	0.32	0.05	0.02	0.28	0.41	0.04
PC(38:4)	0.00	**0.15**	0.58	0.09	0.04	0.85	0.67	0.11
11β-PGE_2	0.00	**0.16**	0.61	0.10	0.05	1.00	0.76	0.15
LPI (16:1)	0.01	**0.16**	0.63	0.10	0.06	1.00	0.86	0.24
LPE(16:1)	0.01	**0.16**	0.63	0.10	0.06	1.00	0.82	0.20
Cysteine	0.00	**0.16**	0.58	0.09	0.04	0.82	0.67	0.11
CE(18:3)	0.00	**0.16**	0.63	0.10	0.06	1.00	0.80	0.18
TG(58:10)	0.00	**0.17**	0.61	0.10	0.05	1.00	0.73	0.13
PE(36:4)	0.01	**0.17**	0.63	0.10	0.06	1.00	0.86	0.24
S-Methylcysteine	0.00	**0.17**	0.63	0.10	0.06	1.00	0.82	0.20
SM(d18:1/24:2)	0.01	**0.17**	0.67	0.11	0.08	1.00	0.91	0.33

Cer(d18:1/24:0)	0.00	**0.17**	0.61	0.10	0.05	1.00	0.76	0.15
LPE (22:5)	0.01	**0.17**	0.63	0.10	0.06	1.00	0.85	0.23
DGLEA	0.01	**0.17**	0.68	0.11	0.08	1.00	0.93	0.35

Comparison of adjusted *P*-value results from different multiple testing procedures in the HUU vs. Long-cART-HEU group overall significance test on the shortlisted biochemicals. The resampling-based FDR adjusted *P*-values used in the main text are included in bold font.
Note: * Li & Ji effective dimension is 40 here (as opposed to total dimension 304).
FDR: False Discovery Rate; FWER: Family-wise error rate; PC: phosphatidylcholines; Cer: ceramide; SM, sphingomyelin; 11β-PGE_2, 11β-prostaglandin E_2; LPI: lysophosphatidylinositol; LPE: lysophosphatidylethanolamine; CE: cholesterol ester; TG: triglyceride; PE: phosphatidylethanolamine; DGLEA: dihomo-γ-linolenic acid.

Supplemental Table 3. Maternal and child demographic variables

Maternal	**HIV neg (n=12)**	**Medium-cART (n=12)**	**Long-cART (n=14)**	**Significance**
Clinical Variables	**Median (Q1,Q3)**	**Median (Q1,Q3)**	**Median (Q1,Q3)**	
Age [y]	31.5 (25.0, 35.5)	27.5 (24.5, 32.5)	28.5 (26.3, 32.0)	NS
Height [cm]	164.5 (161.3, 170.0)	159.5 (157.9, 164.8)	161.0 (160.0, 164.1)	NS
Weight upon inclusion [kg]	75.5 (66.0, 82.9)	66.5 (63.9, 71.3)	69.0 (64.3, 72.5)	NS
BMI	27.2 (25.4, 29.5)	26.0 (23.1, 28.1)	26.7 (24.9, 27.3)	NS
MUAC	32.0 (29.4, 33.3)	27.5 (25.5, 29.6)	28.0 (27.0, 29.8)	*
Parity	2.0 (1.0, 3.3)	2.0 (1.0, 2.3)	1.0 (1.0, 2.0)	NS
Gravidity	3.0 (2.0, 4.3)	3.0 (2.0, 3.3)	2.0 (2.0, 3.8)	NS
Systolic blood pressure	116 (110, 123)	108 (100, 117)	100 (98, 110)	*
Diastolic blood pressure	70 (67, 79)	71 (59, 75)	61 (60, 70)	NS
Non-fasted glucose [mmol/L]	4.2 (4.1, 5.5)	4.0 (3.9, 4.2)	4.5 (4.2, 5.2)	NS
Glycated hemoglobin [µmol/L]	5.2 (4.7, 5.7)	5.3 (4.6, 5.7)	5.2 (4.9, 5.8)	NS
Triglycerides [mmol/L]	2.0 (1.8, 2.6)	1.7 (1.6, 2.0)	1.9 (1.4, 2.5)	NS
High density lipoprotein [mmol/L]	1.2 (0.8, 1.3)	1.6 (1.2, 1.8)	2.0 (1.6, 2.3)	*
Alkaline phosphatase [U/L]	160.0 (128.3, 173.5)	109.0 (89.3, 132.3)	107.0 (89.8, 137.5)	NS
Low density lipoprotein[mmol/L]	2.7 (2.4, 3.7)	3.2 (2.7, 3.5)	3.1 (2.6, 3.6)	NS
Albumin [g/L]	34.5 (33.0, 36.3)	33.5 (31.0, 36.5)	35.5 (33.3, 37.8)	NS
Total protein [g/L]	66.0 (61.8, 68.8)	72.5 (69.5, 78.3)	73.0 (68.8, 74.0)	*
Gamma glutamyl transferase [U/L]	14.0 (8.0, 26.0)	15.0 (10.3, 24.3)	22.5 (17.8, 31.8)	NS
Cholesterol [mmol/L]	4.5 (3.9, 5.1)	4.9 (4.4, 5.7)	5.2 (4.9, 5.8)	NS
Hemoglobin [g/dL]	11.5 (10.0, 12.7)	11.1 (10.4, 11.6)	11.0 (10.0, 11.4)	NS
Platelets [g/dL]	229.0 (198.5, 281.0)	230.5 (177.8, 254.5)	251.0 (188.0, 325.0)	NS
cART initiation time until birth [d]	0 (0, 0)	75 (69, 117)	1003 (574, 1654)	*
Viral load [copies/mL]	N/A	71(15, 6460)	0 (0, 15)	*
CD4+ T cell count [× 10^6 cells/L]]	N/A	475 (328, 603)	521 (444, 586)	NS

Child	HUU (n=12)	Medium-cART-HEU (n=12)	Long-cART-HEU (n=14)	Significance
Clinical Variables	**Median (Q1,Q3)**	**Median (Q1,Q3)**	**Median (Q1,Q3)**	
Gestation [wk]	39.6 (38.7, 42.1)	39.6 (38.4, 41.1)	40.7 (38.5, 42.4)	NS
Sex [a] (male/female; [n])	3/9	6/6	8/6	NS
APGAR-score	9 (9, 10)	9 (9, 10)	9 (9, 10)	NS
MUAC	N/A	13.0 (12.7, 14.0)	13.0 (13.0, 13.5)	NS
Length [cm] at birth	50.0 (49.0, 52.0)	49.0 (48.0, 50.3)	49.5 (48.0, 50.0)	NS
Head circumference [cm] at birth	34.0 (34.0, 36.0)	34.0 (33.0, 34.0)	35.0 (33.3, 35.8)	NS
Birth weight [kg]	3.3 (3.0, 3.7)	3.1 (2.9, 3.5)	3.2 (2.5, 3.6)	NS
Breastfeeding duration (EI) [d]	80 (71, 108)	93 (79, 101)	73 (58, 79)	NS
Breastfeeding duration (LI) [d]	378 (369, 380)	370.5 (350, 384)	370 (364, 404)	NS

[a] represents Chi-squared test; the rest are using Kruskal-Wallis test
*represents *P*-values (<0.05) from Kruskal-Wallis and Chi-squared tests for independence of cART exposure groups in continuous respectively nominal clinical variables.
cART: combinational antiretroviral therapy; NS: Non-significant; Q1: first quartile; Q3: third quartile; BMI: body mass index; MUAC: middle upper arm circumference.

Supplemental Table 4. Pearson correlation analysis showing correlation coefficients of infant metabolites at birth with (r) ≥ 0.5 or ≤ -0.5 with maternal virological and immunological parameters

Metabolites	Virological and immune parameters	Correlation coefficient (r)	*P*-value
L-Methionine	CD4 count	0.54	0.015
CE(18:3)	CD4 count	-0.59	0.006
Cysteine	Viral load	-0.61	0.005
20-hydroxy-PGE_2	BCA1	-0.53	0.002
SM(d18:1/23:1)	IL-10	-0.53	0.003
LPE(20:3)	MCP1	-0.52	0.003
SM(d18:1/24:2)	IL-1β	-0.54	0.002
SM(d18:1/23:1)	IL-1β	-0.57	0.001
DGLEA	IL-12p70	0.54	0.002
Cer(d18:1/23:0)	IL-2	-0.54	0.002
SM(d18:1/23:1)	IL-2	-0.58	0.001

CE: cholesterol ester; 20-hydroxy-PGE_2: 20-hydroxy-prostaglandin E_2; SM, sphingomyelin; LPE: lysophosphatidylethanolamine; DGLEA: dihomo-γ-linolenic acid; Cer: ceramide.

Supplemental Table 5. Pearson correlation analysis showing correlation coefficients of infant metabolites with (r) ≥0.5 or ≤-0.5 with infant cytokines in late infancy

Metabolites	Immune parameters	Correlation coefficient (r)	P-value
CE(18:3)	MCP3	-0.53	0.004
PE(36:4)	BDNF	0.53	0.003
Cer(d18:1/22:0)	IL-27	0.57	0.001
Cer(d18:1/24:0)	IL-27	0.54	0.002
PE(36:4)	TNF	0.60	0.001

CE: cholesterol ester; PE: phosphatidylethanolamine; Cer: ceramide.

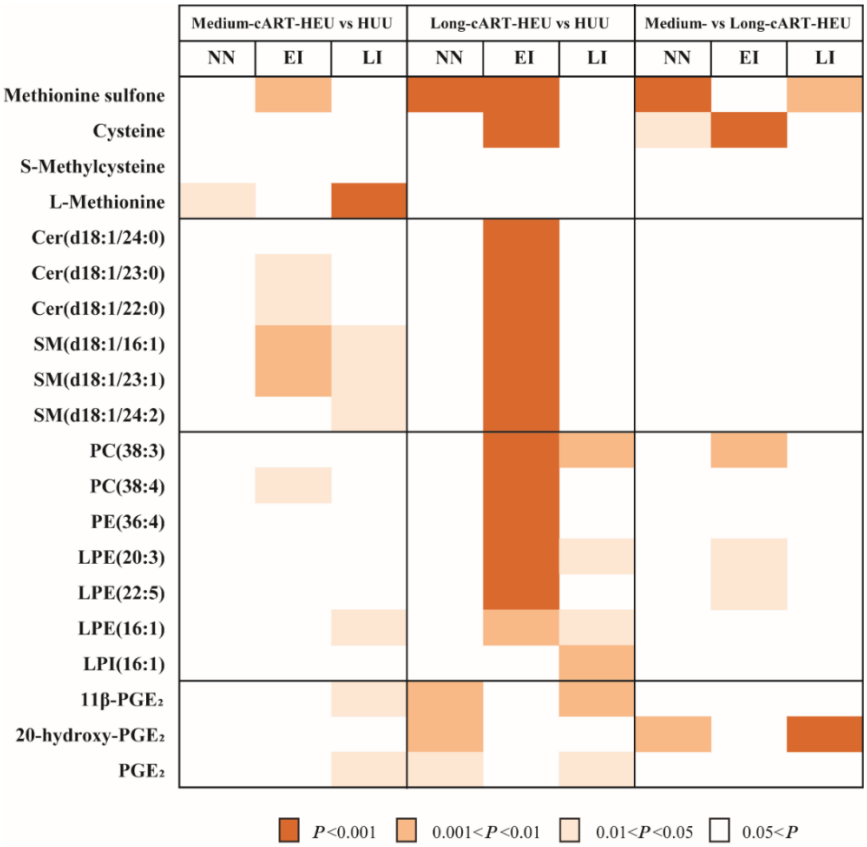

Supplemental Figure 1. Heatmap of corresponding effect size raw *P*-value from the univariate linear mixed model in infant cohort at ages. NN: neonate; EI: early infancy; LI: late infancy; Cer: ceramide; SM, sphingomyelin; PC: phosphatidylcholines; PE: phosphatidylethanolamine; LPE: lysophosphatidylethanolamine; LPI: lysophosphatidylinositol; 11β-PGE_2:11β-prostaglandin E_2; 20-hydroxy-PGE_2: 20-hydroxy-prostaglandin E_2; PGE_2: prostaglandin E_2

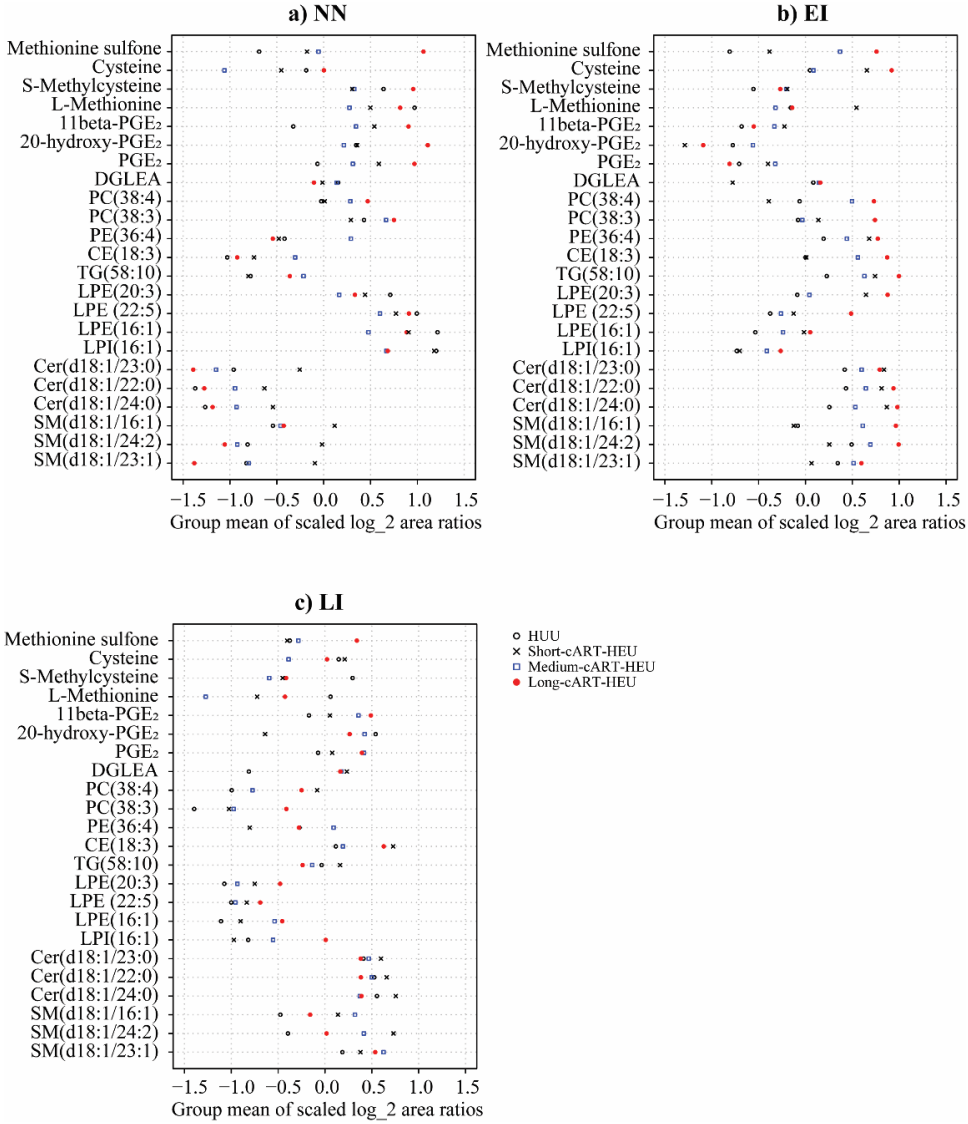

Supplemental Figure 2. Group means of scaled log_2 area ratios of metabolites identified in the overall univariate linear mixed model (shown in Table 1) in children. The Short-cART-HEU group means are included as black crosses (x), the HUU-children (black open circles), Medium-cART-HEU (blue open squares) and Long-cART-HEU (red closed circles) exposure group means illustrated before. NN: neonate; EI: early infancy; LI: late infancy; 11β-PGE_2:11β-prostaglandin E_2; 20-hydroxy-PGE_2: 20-hydroxy-prostaglandin E_2; PGE_2: prostaglandin E_2; DGLEA: dihomo-γ-linolenic acid; PC: phosphatidylcholines; PE: phosphatidylethanolamine; CE: cholesterol ester; TG: triglyceride; LPE: lysophosphatidylethanolamine; LPI: lysophosphatidylinositol; Cer: ceramide; SM, sphingomyelin.

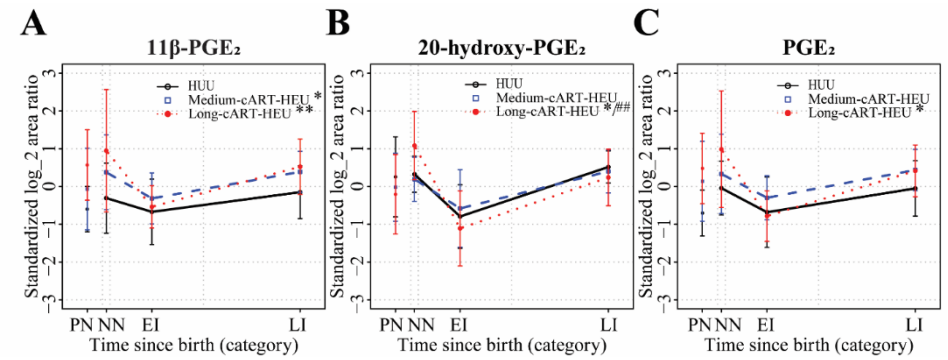

Supplemental Figure 3. Longitudinal trajectories of Prostaglandin E_2 metabolites in children and their paired maternal prenatal samples. (A)11β-PGE_2; (B) 20-hydroxy-PGE_2; (C) PGE_2. The points represent the means of the standardized, log_2 area ratios per age category for the exposure groups (black open circles represent HUU group, blue open squares represent Medium-cART-HEU group and red solid circles represent Long-cART-HEU group) (NN: Neonate; EI: early infancy; LI: late infancy). The lines connecting the points are interpolations. The maternal prenatal "PN" exposure group means are included as disconnected points at the left-hand side of each figure. *represent the corresponding significance level of the raw *P*-value of group comparisons to HUU from the univariate linear mixed model in the infant cohort (***P <0.001, **P <0.01, *P <0.05); $^{\#}$represent the corresponding significance level of the raw *P*-value of group comparisons to medium-cART-HEU group from the univariate linear mixed model in the infant cohort ($^{\#\#}P$ <0.01, $^{\#}P$ <0.05). The specific raw *P*-values are furthermore listed in Table 1. 11β-PGE_2:11β-prostaglandin E_2; 20-hydroxy-PGE_2: 20-hydroxy--prostaglandin E_2; PGE_2: prostaglandin E_2.

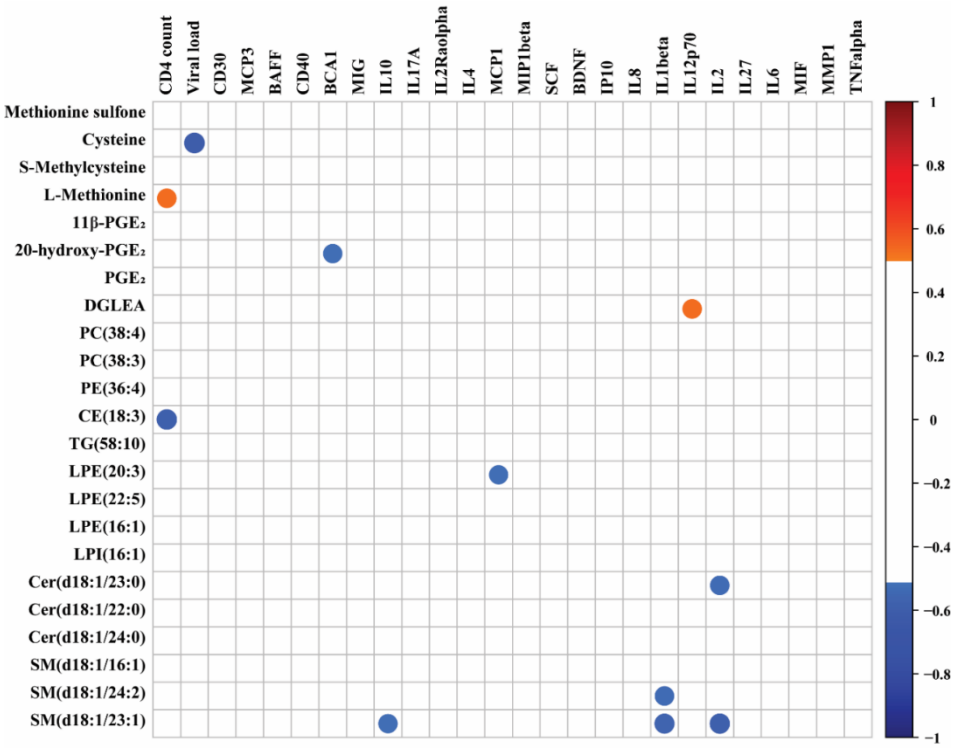

Supplemental Figure 4. Heatmap of Pearson correlations of infant metabolites at birth (rows) with maternal virological and immunological parameters during pregnancy (columns). Color intensity represents the correlation coefficients (red represents positive correlations; blue represents negative correlations). Correlations shown with (r) ≥0.5 or ≤-0.5. 11β-PGE_2:11β-prostaglandin E_2; 20-hydroxy-PGE_2: 20-hydroxy-prostaglandin E_2; PGE_2: prostaglandin E_2; DGLEA: dihomo-γ-linolenic acid; PC: phosphatidylcholines; PE: phosphatidylethanolamine; CE: cholesterol ester; TG: triglyceride; LPE: lysophosphatidylethanolamine; LPI: lysophosphatidylinositol; Cer: ceramide; SM, sphingomyelin.

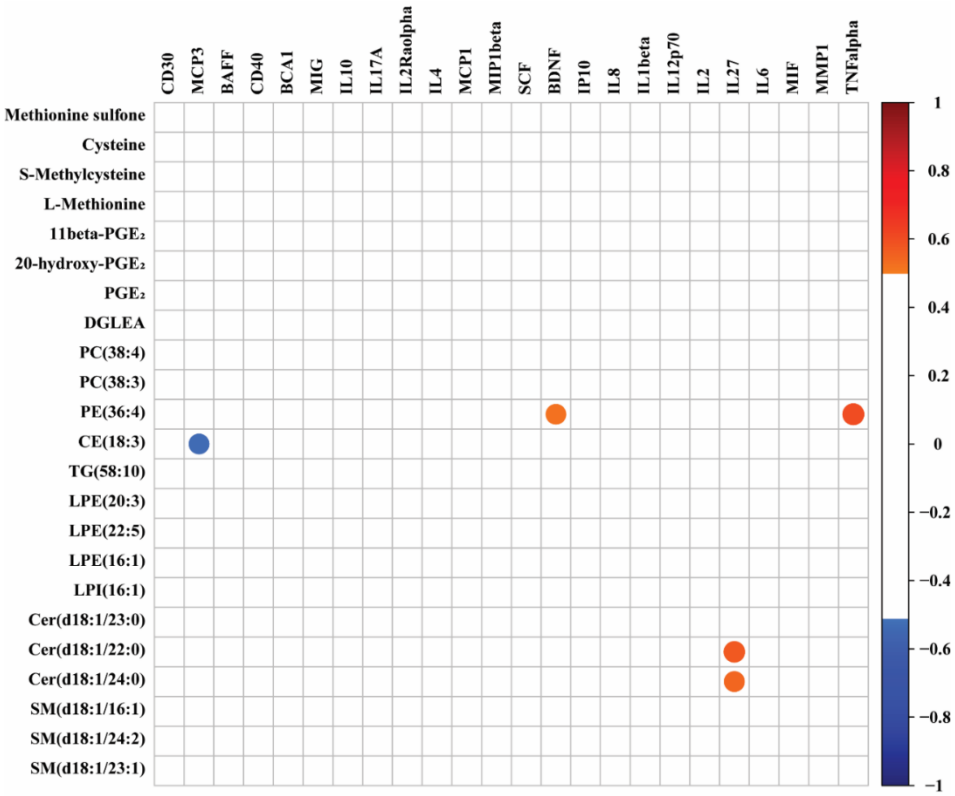

Supplemental Figure 5. Heatmap of Pearson correlations of infant metabolites (rows) with immunological mediators (columns) in late infancy. Color intensity represents the correlation coefficients (red represents positive correlations; blue represents negative correlations). Correlations shown with (r) ≥0.5 or ≤-0.5. 11β-PGE_2:11β-prostaglandin E_2; 20-hydroxy-PGE_2: 20-hydroxy-prostaglandin E_2; PGE_2: prostaglandin E_2; DGLEA: dihomo-γ-linolenic acid; PC: phosphatidylcholines; PE: phosphatidylethanolamine; CE: cholesterol ester; TG: triglyceride; LPE: lysophosphatidylethanolamine; LPI: lysophosphatidylinositol; Cer: ceramide; SM, sphingomyelin.